

Comparison of CMS measurements with predictions at NLO applying the Parton Branching Method and PYTHIA

Fernando Guzman ¹, Si Hyun Jeon ¹, Hannes Jung ¹, Danyer Perez Adan ¹,
Sara Taheri Monfared ¹, Fateme Almaksusi ², Daniel Belmonte Perez ²,
Dorukhan Boncukcu ², Aleksandr Boger ², Emmanuel Botero Osorio ²,
Isadora Bozza Galvão ², Juan Esteban Ospina Holguin ², Behnam Falahi ²,
Faeze Gagonani ², Omar Gonzalez ², Acelya Deniz Güngördü ²,
Abdelhamid Haddad ², Mahtab Jalalvandi ², Josue Daniel Jaramillo ²,
Jesus Jimenez Zepeda ², Gleb Kutyrév ², Nazanin Zahra Noroozi ²,
Nestor Raul Mancilla Xinto ², Haritz Mentaste ²,
Lucas Johnny Monte Tamayo ², Fernanda Mora Rey ²,
Inmaculada Moyano-Rejano ², Vibha Padmanabhan ², Mayvi Pedraza ²,
Swapnil Rathore ², Cristina Ruiz Gonzalez ², Caue E. Sousa ²,
Quratulain Zahoor ², and Haoliang Zheng ²

¹Supervisor

²Summerstudent

Abstract

In August 2023, more than 30 students joined the *Special Remote DESY summer-school* to work on projects of importance for LHC experiments. In a dedicated initiative, analyses that had not been incorporated into the RIVET package were implemented and verified. Here, a brief description of the accomplished work is given, and a comparison of the measurements with predictions obtained from matched standard parton shower Monte Carlo event generators as well as with those obtained from Parton-Branching TMDs with corresponding parton showers are presented.

1 Introduction

In August 2023, more than 30 students participated the *Special Remote DESY summer-school* [1] to work on projects of importance for LHC experiments. The *Special Remote DESY summer-school* was endorsed by IUPAP [2] and included in the program of the International Year of Basic Sciences for Sustainable Development (IYBSSD) [3]. The school was fully online, with virtual meeting sessions from 2-4 pm CEST, for students from the far East it was late in the evening and for students from the far West it was very early in the morning. A similar fully online school was held in 2021 [4].

The school in 2023 was held in the spirit of the IUPAP policy to *“open the channels for scientific cooperation across all political and other divides in the hope and expectation that enhanced scientific collaborations are an important means to develop improved understandings between different peoples that contributes to world peace”*.

The student projects were on coding, testing and validating computer codes of experimental analyses which have been already published by the CMS collaboration, but are not yet available in the Rivet (Robust Independent Validation of Experiment and Theory) package [5].

In the following, we describe briefly the analyses in the area of QCD jets and electro-weak physics, which have been developed.

2 New Rivet plugins

Several published results obtained with the CMS experiment at the LHC, which were not yet implemented in the Rivet package were investigated, ranging from jet production at $\sqrt{s} = 7$ TeV, over heavy flavor production to measurements involving the electroweak (EW) bosons γ, Z at $\sqrt{s} = 13$ TeV. The theoretical predictions at leading order (LO), obtained with PYTHIA8 [6–8], using the CUETM1 tune [9] to fix a number of free parameters sensitive to the treatment of the underlying event, were used to validate the implementation of the different analyses into the Rivet package, and to compare the obtained results with those shown in the original publications.

The following analyses were studied:

- CMS_2010_I878118 Prompt and Non-Prompt J/ψ Production in pp Collisions at $\sqrt{s} = 7$ TeV [10] (Mayvi Pedraza Monzon, Supervisor: F. Guzman)
- CMS_2011_I944755 J/ψ and ψ_{2S} production in pp collisions at $\sqrt{s} = 7$ TeV [11] (Shijie Zhang, Supervisor: H. Jung)
- CMS_2011_I895742 Measurement of the differential dijet production cross section in proton-proton collisions at $\sqrt{s} = 7$ TeV [12] (Josué Daniel Jaramillo Arroyave, Fernanda Mora Rey, Supervisor: H. Jung)

- CMS_2012_I1093951 Measurement of the Inclusive Cross Section $\sigma(pp \rightarrow b\bar{b}X \rightarrow \mu\mu X')$ at $\sqrt{s} = 7$ TeV [13] (Faeze Gagonani, Nestor Raul Mancilla Xinto, Supervisor: H. Jung)
- CMS_2015_I1345159 Distributions of Topological Observables in Inclusive Three- and Four-Jet Events in pp Collisions at $\sqrt{s} = 7$ TeV [14] (Dorukhan Boncukcu, Acelya Deniz Güngördü, Supervisor: H. Jung)
- CMS_2015_I1359450 Measurement of the Z boson differential cross section in transverse momentum and rapidity in proton-proton collisions at 8 TeV [15] (Emmanuel Botero Osorio, Jesus Jimenez-Zepeda, Nazanin Zahra Norouzi, Juan Esteban Ospina, Swapnil Rathore, Supervisor: S. Taheri Monfared)
- CMS_2015_I1410826 Measurement of the inclusive jet cross section in pp collisions at $\sqrt{s} = 2.76$ TeV [16] (Vibha Padmanabha, Quratulain Zahoor, Supervisor: H. Jung)
- CMS_2016_I1485195 Measurement of the total and differential inclusive B^+ hadron cross sections in pp collisions at $\sqrt{s} = 13$ TeV [17] (Lucas Tamayo, Supervisor: H. Jung)
- CMS_2019_I1757506 Study of J/ψ meson production inside jets in pp collisions at $\sqrt{s} = 8$ TeV [18] (Behnam Falahi, Supervisor: H. Jung)
- CMS_2021_I1876550 Measurement of prompt open-charm production cross sections in proton-proton collisions at $\sqrt{s} = 13$ TeV [19] (Fateme Almaksusi, Haoliang Zheng, Supervisor: H. Jung)
- CMS_2021_I1869513 Measurement of the electroweak production of $Z\gamma$ and two jets in proton-proton collisions at $\sqrt{s} = 13$ TeV and constraints on anomalous quartic gauge couplings [20] (Daniel Belmonte, Haritz Mentaste, Omar González, Supervisor: Si Hyun Jeon)
- CMS_2021_I1876311 Measurements of the electroweak diboson production cross sections in proton-proton collisions at $\sqrt{s} = 5.02$ TeV using leptonic decays [21] (Cristina Ruiz Gonzalez, Inmaculada Moyano-Rejano, Supervisor: Si Hyun Jeon)
- CMS_2021_I1949191 Measurement of the inclusive and differential WZ production cross sections, polarization angles, and triple gauge couplings in pp collisions at $\sqrt{s} = 13$ TeV [22] (Mahtab Jalalvandi, Supervisor: D. Perez Adan)
- CMS_2021_I1992937 Measurement of the production cross section for Z+b jets in proton-proton collisions at $\sqrt{s} = 13$ TeV [23] (Caue E. Sousa, Gleb Kutyrev, Aleksandr Boger, Isadora Bozza Galvão, Abdelhamid Haddad, Supervisor: D. Perez Adan)

3 Comparison with predictions

While predictions at leading order (LO) obtained with PYTHIA8 were used to test and validate the coded analyses, we present here a comparison of theoretical predictions obtained at next-to-leading (NLO) in the strong coupling α_s .

At NLO, the MADGRAPH5_AMC@NLO package [24] was used to calculate the hard process and supplement the partonic processes with parton shower and hadronization. We use the NLO Parton Branching (PB) collinear and the transverse momentum dependent (TMD) parton distributions as obtained in Ref. [25] from QCD fits to precise DIS (Deep Inelastic Scattering) data from HERA [26] using the xFitter analysis framework [27, 28]. We cross check the results with predictions using the NNPDF31 collinear parton distributions [29]. We apply the Parton Branching transverse momentum distributions (TMD) PB-NLO-2018-Set 2 together with the TMD parton shower for the initial state as implemented in CASCADE3 [30] (labelled MCatNLO+CAS3) as well as a standard parton shower obtained with PYTHIA8 (labelled MCatNLO+PYTHIA8). The NLO hard process is calculated with appropriate subtraction terms for the use with CASCADE3 and PYTHIA8. We use μ_{def} as factorization and renormalization scale $\mu_{def} = \mu_{R,F} = \frac{1}{2} \sum_i \sqrt{m_i^2 + p_{t,i}^2}$, where the index i runs over all particles in the matrix element final state.

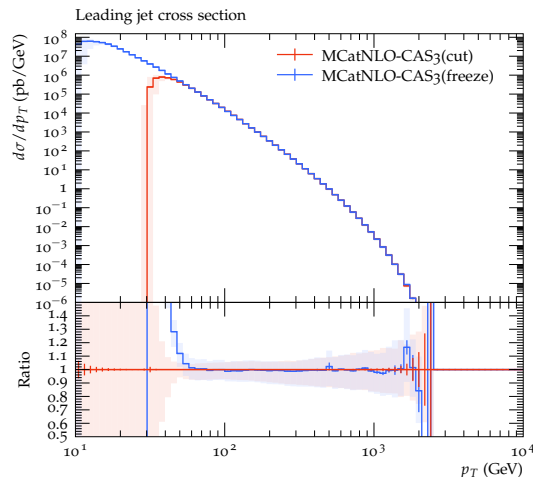


Figure 1: Differential cross section as a function of the leading jet p_T obtained with MCatNLO+CAS3 applying to freeze of the scale (see eq.(1)) and with a cutoff of $p_T > 30$ GeV.

Since some measurements are performed at very small transverse momenta, special care has to be taken to avoid instabilities of the NLO cross section as well as to avoid too large negative cross sections. We apply a taming factor for the scale $\mu_{R,F}$:

$$\mu = \mu_{R,F} = \mu_{def}^2 + \mu_0^2, \quad (1)$$

with μ_{def} being the default scale and μ_0 being a free parameter to avoid too small scales. We found the $\mu_0 = 20$ GeV leads to stable results for jet production with a transverse momentum down to $p_T \sim 10$ GeV.

In Fig. 1 we show a comparison of the cross section as a function of the leading jet p_T calculated with and without the taming factor of eq.(1). We do not observe any significant change in the cross section at larger p_T , however, applying eq.(1) we are able to use an NLO calculation for jet production down to $p_T \sim 10$ GeV.

The theoretical uncertainty is estimated by independent variation of the factorization and renormalization scales by a factor of two up and down, avoiding the extreme combinations (7-point variation) and it is shown by the band in the figures.

In all predictions, we do not consider effects from multiparton interactions.

3.1 Comparison to QCD measurements

In Figs. 2–4 we compare measurements from CMS with predictions obtained from MCatNLO+CAS3 and MCatNLO+PYTHIA8 using dijet production at NLO. The aim of this comparison is to check for differences in predictions from MCatNLO+CAS3 and MCatNLO+PYTHIA8, since both predictions are based on different assumptions for higher order corrections in the form of parton showers. In general we observe a rather good agreement between the two different predictions.

In Fig. 2 inclusive jet cross sections are shown, the calculations give very similar predictions, since inclusive jet and dijet production is largely sensitive to the collinear parton distributions. Also the prediction using NNPDF31 agrees well with the others.

In the following distributions the effect of TMD parton densities and parton shower is investigated. In Fig. 3(left) the invariant mass distribution of four-jet events with a p_T of the leading jet of $190 < p_T < 300$ GeV is shown. The four-jet mass distribution is sensitive to the parton shower, since in the dijet matrix element at NLO at most three jets are produced, and therefore the fourth jet comes from parton shower. In Fig. 3(right) the particle content of jet evolution is investigated by a measurement of the energy of J/ψ mesons inside jets with a transverse momentum of $p_T > 25$ GeV at $\sqrt{s} = 8$ TeV. The predictions are in good agreement with the measurements.

Next, heavy flavor production is studied. In Fig. 4 measurements of charm and bottom production are shown. Since heavy quarks are not only produced in the hard matrix element, but also during the jet evolution, we use the zero-mass-variable-flavor-number scheme (ZMVFS) for the calculation (which allows charm or bottom quarks to be produced from light parton matrix elements). However, a drawback of ZMVFS is, that the matrix element becomes divergent for small p_T (since all partons are treated massless), and therefore a p_T cut-off has to be applied. For NLO calculations with subtraction terms (in the MCatNLO frame), we found, that we need to freeze the scale μ for low p_T . With the procedure described in eq.(1) we are able to use ZMVFS at NLO down to $p_T = 10$ GeV. One can clearly see the effect of this lower p_T -cut in the distributions of the transverse momentum of heavy flavoured mesons in Fig. 4. Apart from the low p_T -region, which is affected by the p_T cut,

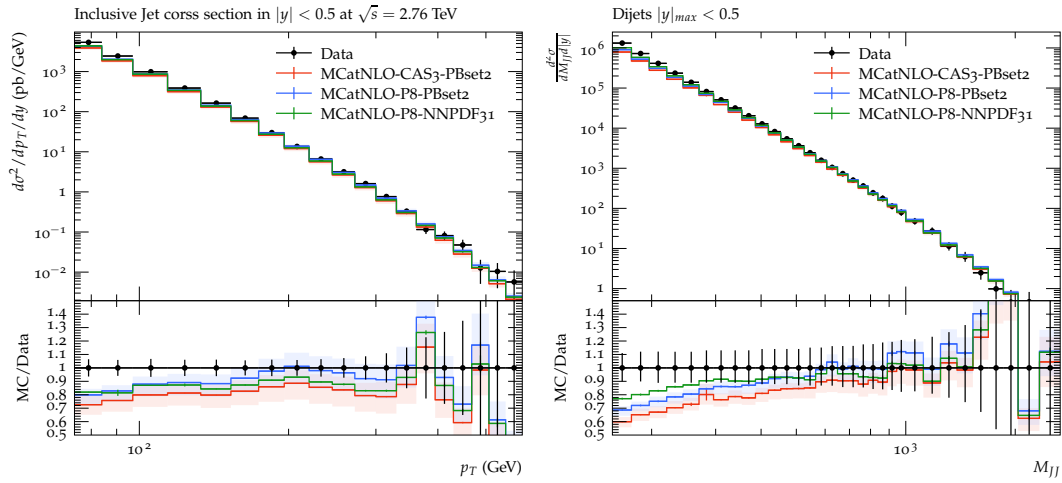


Figure 2: Differential cross section as a function of the jet p_T at $\sqrt{s} = 2.76$ TeV [16] (left) and as a function of the dijet mass M_{JJ} at $\sqrt{s} = 7$ TeV [12] (right) obtained with MCatNLO+CAS3 and MCatNLO+PYTHIA8 using PB-NLO-2018-Set 2. For comparison also shown is MCatNLO+PYTHIA8 with NNPDF31.

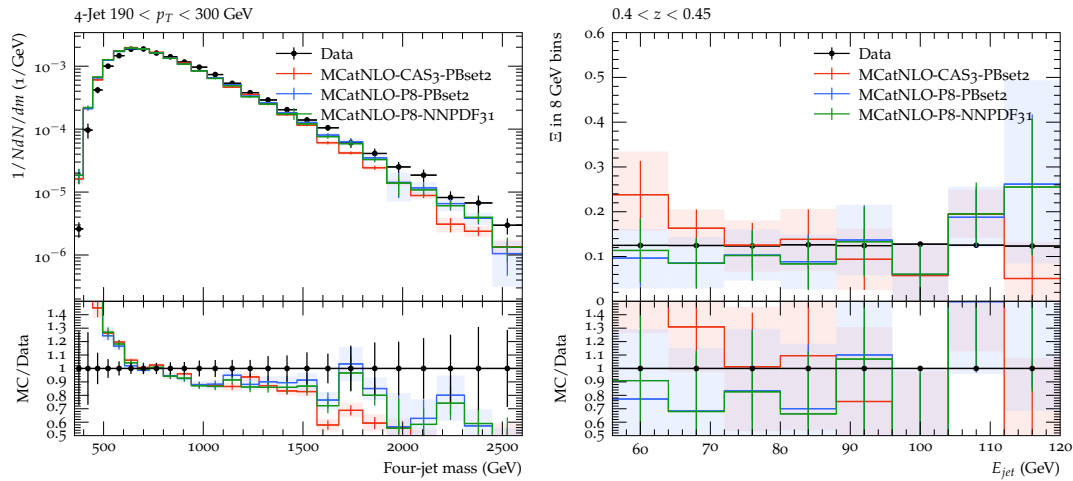


Figure 3: Normalized distribution for x_3 in high p_T three-jet events at $\sqrt{s} = 7$ GeV [14] (left) and the normalized distribution of energy of J/ψ mesons inside jets at $\sqrt{s} = 8$ GeV [18] (right) obtained with MCatNLO+CAS3 and MCatNLO+PYTHIA8 using PB-NLO-2018-Set 2, for comparison also shown is MCatNLO+PYTHIA8 with NNPDF31

the predictions agree rather well with the measurements and only small differences between the different parton shower approaches are observed.

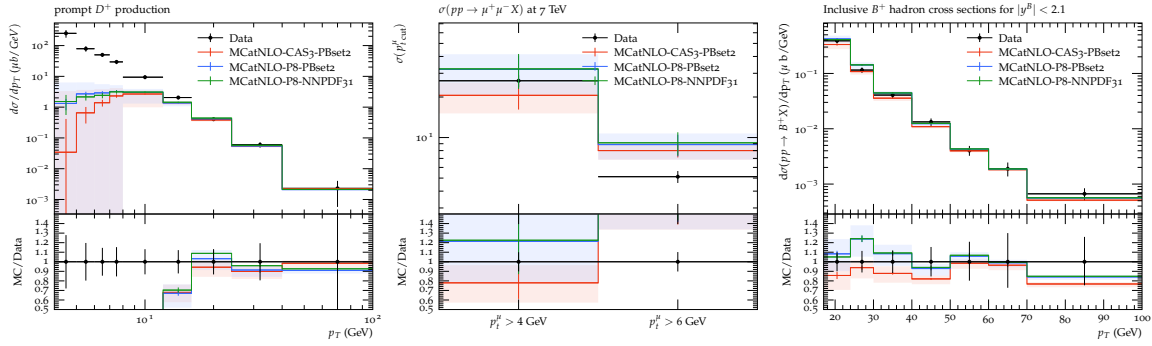


Figure 4: Differential cross section as a function of p_T for D^* production at $\sqrt{s} = 13$ TeV [19] (left), the total cross section for $\sigma(pp \rightarrow b\bar{b}X \rightarrow \mu\mu X')$ at $\sqrt{s} = 7$ TeV as a function of the p_T cut (middle) [13] and the differential cross section for B^+ mesons at $\sqrt{s} = 13$ TeV [17] (right) obtained with MCatNLO+CAS3 and MCatNLO+PYTHIA8 using PB-NLO-2018-Set 2, for comparison also shown is MCatNLO+PYTHIA8 with NNPDF31.

3.2 Comparison to Onium processes

Measurements of J/ψ production have been performed in [10, 11]. We use the CASCADE Monte Carlo event generator [30–32] in standalone mode with internally implemented processes based on k_T -factorization with the un-integrated gluon density JH-2013-set1 [33]. Prompt J/ψ and $\psi(2S)$ are calculated within the color singlet model, as well as χ_c production for feed-down to J/ψ . A description of the calculation is given in Ref. [34]. The non-

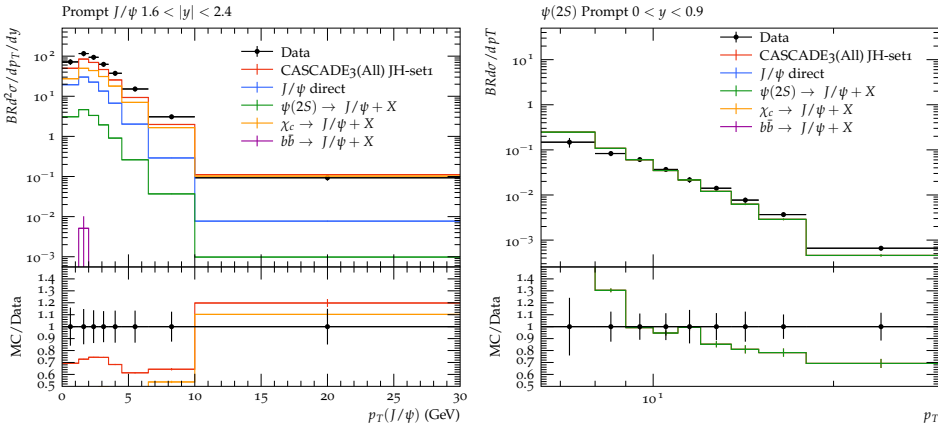


Figure 5: Double differential cross section for J/ψ production at $\sqrt{s} = 7$ TeV [10] (left), and for $\psi(2S)$ production [11] (right) compared with predictions from CASCADE3.

prompt production J/ψ is generated using $g^* g^* \rightarrow b\bar{b}$ with subsequent decay to J/ψ via the

hadronization package PYTHIA6. In Fig. 5, we show the double differential cross section for prompt J/ψ production [10] as well as the cross section for prompt $\psi(2S)$ production [11]. A rather good description of the measurements with the predictions based on k_T -factorization is achieved.

3.3 Comparison to Electroweak processes

In this section we compare measurements of electroweak processes with predictions from MCatNLO+CAS3 and MCatNLO+PYTHIA8 (with the same settings for parton densities and parton showers as in the previous section) using DY production at NLO.

In Fig. 6(left) the transverse momentum of Z bosons at $\sqrt{s} = 8$ TeV is shown. The calculations give similar predictions. At larger p_T the predictions fall below the measurements, since at larger p_T higher order corrections become important.

In Fig. 6(right) the cross section as a function of the azimuthal angle $\Delta\phi$ between a b-jet and the Z boson in Z+b events at $\sqrt{s} = 13$ is shown. Here we compare predictions obtained with inclusive Z boson production at NLO with the measurements and the difference of the predicted cross section to the measurement, especially at small $\Delta\phi$, can be attributed to higher order hard jet radiation, which is not included in the simulation. Small differences between the parton shower and the TMD predictions can be observed.

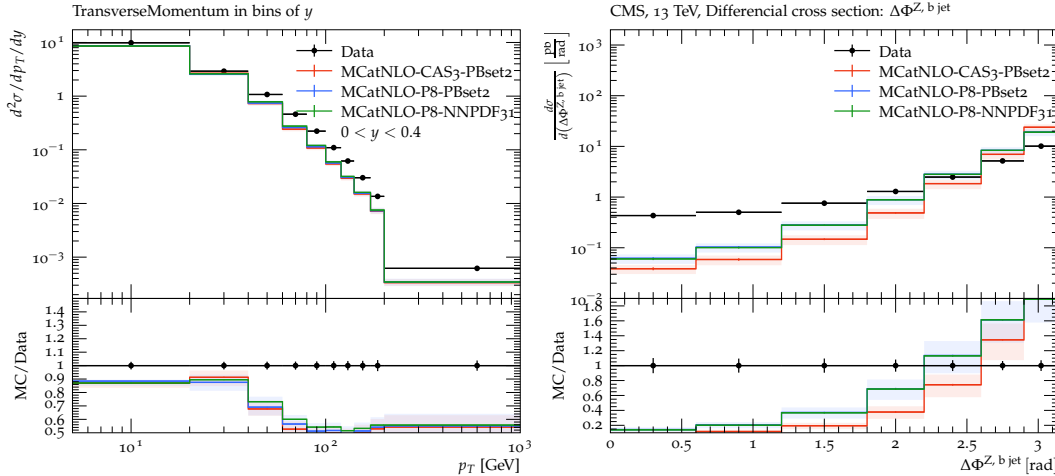


Figure 6: Differential cross section as a function of p_T for Z production at $\sqrt{s} = 8$ TeV [15] (left), and as a function of the azimuthal angle $\Delta\phi$ between a b-jet and the Z boson in Z+b events at $\sqrt{s} = 13$ TeV [23] (right) obtained with MCatNLO+CAS3 and MCatNLO+PYTHIA8 using PB-NLO-2018-Set 2. For comparison also shown is MCatNLO+PYTHIA8 with NNPDF31.

In Fig. 7(left) the total cross section of ZZ production as a function of \sqrt{s} as measured in [21] is compared with predictions obtained from calculations obtained with a hard process of $\rightarrow ZZ + X$ at NLO with MCatNLO+CAS3 and MCatNLO+PYTHIA8.

In Fig. 7(right) the jet multiplicity in WZ events is shown. The hard process is calculated in the mode $Z \rightarrow l\nu l^+l^-$ with MADGRAPH5_AMC@NLO. Differences coming from the different parton showers can be observed in the jet multiplicity.

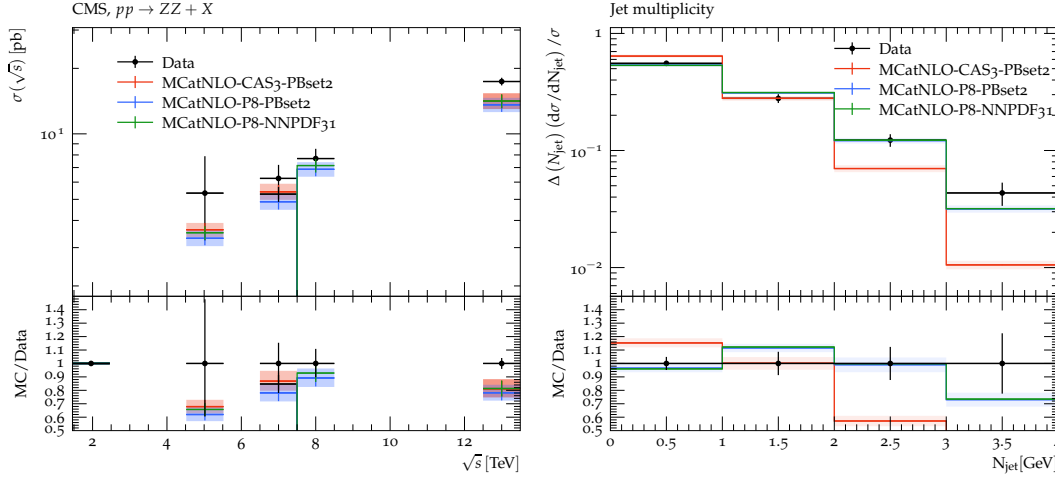


Figure 7: Measurements di-boson production compared with predictions obtained with MCatNLO+CAS3 and MCatNLO+PYTHIA8 using PB-NLO-2018-Set 2. Total cross section for ZZ production as a function of \sqrt{s} (left) [21], jet multiplicity for WZ production at $\sqrt{s} = 13$ TeV [22] (right). For comparison also shown is MCatNLO+PYTHIA8 with NNPDF31

In Fig. 8 the cross section for $Z\gamma jj$ at $\sqrt{s} = 13$ TeV [20] as a function of the leading jet p_T is shown for events in the EW phase space (left) and in the full EW+QCD phase space (right). For the prediction, the hard process generated is $Z+2jet$ at NLO, the photon is radiated as part of the final state parton shower, thus representing only the pure QCD phase space. A significant difference between the predictions of MCatNLO+CAS3 and MCatNLO+PYTHIA8 is observed, which can be attributed to the treatment of high p_T photon radiation in the parton shower.

4 Conclusion

During August 2023 students from different countries joined the *Special Remote DESY summer-school* investigating analyses performed by the CMS experiment at the LHC. Several analyses in the QCD and electroweak area were implemented into the Rivet analysis frame for easy comparison with predictions of Monte Carlo event generators.

The analyses were validated by comparing the results of simulations with the ones described in the original publications. The results presented here use the newly coded Rivet plugins to perform a comparison of predictions obtained with MCatNLO+CAS3 based Parton Branching transverse momentum dependent (PB-TMD) parton distributions with the

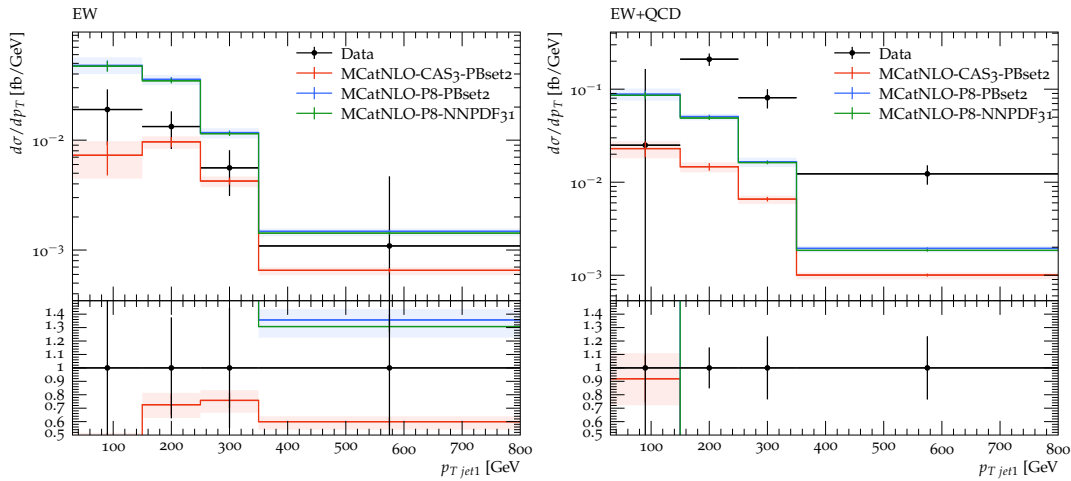


Figure 8: Jet p_T distribution for events in $Z\gamma jj$ events at $\sqrt{s} = 13$ TeV [20] obtained with MCatNLO+CAS3 and MCatNLO+PYTHIA8 using PB-NLO-2018-Set 2. Left: distribution for events in the EW phase space, right: distribution of events in the full EW+QCD phase space.

corresponding parton shower and with MCatNLO+PYTHIA8 applying collinear parton densities and parton showers. The hard processes were generated with MCatNLO at NLO with the collinear parton density PB-NLO-2018-Set 2 (and for comparison NNPDF31). It is observed that the difference between predictions obtained with different collinear parton densities is very small, however in some distributions differences are observed between the conventional parton shower in PYTHIA8 and the TMD based parton shower (and TMD distributions) in MCatNLO+CAS3.

The comparisons presented here are the first systematic comparisons of predictions based on MCatNLO+CAS3 and MCatNLO+PYTHIA8 applying the same collinear parton densities, and therefore contribute to a better understanding of the differences between predictions based on TMD parton densities and conventional parton showers.

The very successful cooperation and collaboration of students with different backgrounds contribute significantly to the Science4Peace idea.

Acknowledgments. We are grateful to Andy Buckley and Christian Gütschow from the Rivet team for their support and advice before, during and after the summer-school. We are also grateful to Markus Seidel for his advice on missing RIVET plugins in CMS as well as for his support in technical details of the analyses. Help and support was also received from Achim Geiser on Onium production as well as from Patrick Connor on jet production analyses in CMS.

References

- [1] “Special Remote DESY summer school 2023”, 2023.
- [2] “Special Remote DESY summer school 2023 (endorsed by IUPAP)”, International Union of Pure and Applied Physics (IUPAP). 2023.
- [3] “Special Remote DESY summer school 2023 (part of IYBSSD)”, International Year of Basic Sciences for Sustainable Development 2022/2023 (IYBSSD). 2023.
- [4] M. I. Abdulhamid et al., “Rivet, RivetHZTool and HERA – A validation effort for coding HERA measurements for Rivet”, *arXiv:2112.12598*.
- [5] C. Bierlich et al., “Robust Independent Validation of Experiment and Theory: Rivet version 3”, *SciPost Phys.* **8** (2020) 026, *arXiv:1912.05451*.
- [6] T. Sjöstrand, S. Mrenna, and P. Z. Skands, “A brief introduction to PYTHIA 8.1”, *Comput. Phys. Commun.* **178** (2008) 852–867, *arXiv:0710.3820*.
- [7] T. Sjöstrand et al., “An introduction to PYTHIA 8.2”, *Comput. Phys. Commun.* **191** (2015) 159, *arXiv:1410.3012*.
- [8] C. Bierlich et al., “A comprehensive guide to the physics and usage of PYTHIA 8.3”, *arXiv:2203.11601*.
- [9] CMS Collaboration, “Event generator tunes obtained from underlying event and multiparton scattering measurements”, *Eur. Phys. J. C* **76** (2016) 155, *arXiv:1512.00815*.
- [10] CMS Collaboration, “Prompt and Non-Prompt J/ψ Production in pp Collisions at $\sqrt{s} = 7$ TeV”, *Eur. Phys. J. C* **71** (2011) 1575, *arXiv:1011.4193*.
- [11] CMS Collaboration, “ J/ψ and ψ_{2S} production in pp collisions at $\sqrt{s} = 7$ TeV”, *JHEP* **02** (2012) 011, *arXiv:1111.1557*.
- [12] CMS Collaboration, “Measurement of the differential dijet production cross section in proton-proton collisions at $\sqrt{s} = 7$ TeV”, *Phys. Lett. B* **700** (2011) 187, *arXiv:1104.1693*.
- [13] CMS Collaboration, “Measurement of the Inclusive Cross Section $\sigma(pp \rightarrow b\bar{b}X \rightarrow \mu\mu X')$ at $\sqrt{s} = 7$ TeV”, *JHEP* **06** (2012) 110, *arXiv:1203.3458*.
- [14] CMS Collaboration, “Distributions of Topological Observables in Inclusive Three- and Four-Jet Events in pp Collisions at $\sqrt{s} = 7$ TeV”, *Eur. Phys. J. C* **75** (2015) 302, *arXiv:1502.04785*.

- [15] CMS Collaboration, “Measurement of the Z boson differential cross section in transverse momentum and rapidity in protonproton collisions at 8 TeV”, *Phys. Lett. B* **749** (2015) 187, arXiv:1504.03511.
- [16] CMS Collaboration, “Measurement of the inclusive jet cross section in pp collisions at $\sqrt{s} = 2.76$ TeV”, *Eur. Phys. J. C* **76** (2016), no. 5, 265, arXiv:1512.06212.
- [17] CMS Collaboration, “Measurement of the total and differential inclusive B^+ hadron cross sections in pp collisions at $\sqrt{s} = 13$ TeV”, *Phys. Lett. B* **771** (2017) 435, arXiv:1609.00873.
- [18] CMS Collaboration, “Study of J/ψ meson production inside jets in pp collisions at $\sqrt{s} = 8$ TeV”, *Phys. Lett. B* **804** (2020) 135409, arXiv:1910.01686.
- [19] CMS Collaboration, “Measurement of prompt open-charm production cross sections in proton-proton collisions at $\sqrt{s} = 13$ TeV”, *JHEP* **11** (2021) 225, arXiv:2107.01476.
- [20] CMS Collaboration, “Measurement of the electroweak production of $Z\gamma$ and two jets in proton-proton collisions at $\sqrt{s} = 13$ TeV and constraints on anomalous quartic gauge couplings”, *Phys. Rev. D* **104** (2021) 072001, arXiv:2106.11082.
- [21] CMS Collaboration, “Measurements of the electroweak diboson production cross sections in proton-proton collisions at $\sqrt{s} = 5.02$ TeV using leptonic decays”, *Phys. Rev. Lett.* **127** (2021), no. 19, 191801, arXiv:2107.01137.
- [22] CMS Collaboration, “Measurement of the inclusive and differential WZ production cross sections, polarization angles, and triple gauge couplings in pp collisions at $\sqrt{s} = 13$ TeV”, *JHEP* **07** (2022) 032, arXiv:2110.11231.
- [23] CMS Collaboration, “Measurement of the production cross section for Z+b jets in proton-proton collisions at $\sqrt{s} = 13$ TeV”, *Phys. Rev. D* **105** (2022), no. 9, 092014, arXiv:2112.09659.
- [24] J. Alwall et al., “The automated computation of tree-level and next-to-leading order differential cross sections, and their matching to parton shower simulations”, *JHEP* **1407** (2014) 079, arXiv:1405.0301.
- [25] A. Bermudez Martinez et al., “Collinear and TMD parton densities from fits to precision DIS measurements in the parton branching method”, *Phys. Rev. D* **99** (2019) 074008, arXiv:1804.11152.
- [26] ZEUS, H1 Collaboration, “Combination of measurements of inclusive deep inelastic $e^\pm p$ scattering cross sections and QCD analysis of HERA data”, *Eur. Phys. J. C* **75** (2015) 580, arXiv:1506.06042.

- [27] xFitter Developers' Team Collaboration, H. Abdolmaleki et al., "xFitter: An Open Source QCD Analysis Framework. A resource and reference document for the Snowmass study", 6, 2022. arXiv:2206.12465.
- [28] S. Alekhin et al., "HERAFitter, Open Source QCD Fit Project", *Eur. Phys. J. C* **75** (2015) 304, arXiv:1410.4412.
- [29] NNPDF Collaboration, "Parton distributions from high-precision collider data", *Eur. Phys. J. C* **77** (2017) 663, arXiv:1706.00428.
- [30] S. Baranov et al., "CASCADE3 A Monte Carlo event generator based on TMDs", *Eur. Phys. J. C* **81** (2021) 425, arXiv:2101.10221.
- [31] H. Jung et al., "The CCFM Monte Carlo generator CASCADE version 2.2.03", *Eur. Phys. J. C* **70** (2010) 1237, arXiv:1008.0152.
- [32] H. Jung, "The CCFM Monte Carlo generator CASCADE", *Comput. Phys. Commun.* **143** (2002) 100, arXiv:hep-ph/0109102.
- [33] F. Hautmann and H. Jung, "Transverse momentum dependent gluon density from DIS precision data", *Nuclear Physics B* **883** (2014) 1, arXiv:1312.7875.
- [34] S. P. Baranov, "Highlights from the kT factorization approach on the quarkonium production puzzles", *Phys. Rev. D* **66** (2002) 114003.